IJAME
Int. J. of Applied Mechanics and Engineering, 2026, vol.31, No.4, pp.59-78
DOI: 10.59441/ijame/224476

FATIGUE ANALYSIS OF AN ELEVATOR DRIVE SHAFT: USING THE ASME AND DE-GOODMAN CRITERIA.

N. LADACI
Department of Technology, Higher Normal School of Technological Education, ENSET-Skikda, ALGERIA
E-mail: naouriladagm@gmail.com

This study considers the drive shaft of a bucket elevator, which is an integral component of a plant mechanism used to transport cement from bottom to top. Failures can occur for various reasons, possibly creating safety problems. This shaft broke during regular operation and without reaching the limit of its service life. Investigations revealed that the leading cause of failure was fatigue caused by a stress concentration phenomenon, where the source is the keyway, and cyclic loading due to power transmission elements such as the left-hand coupling and the middle wheel supporting buckets full of material. This study aimed to determine the leading cause of the failure by checking the shaft diameter according to two criteria, DE-Goodman and ASME, and comparing it with the manufacturer's diameter (*220 mm*). The results showed that the diameter calculated according to the ASME standard is *140 mm*, while that obtained using the DE-Goodman method is *214 mm*.

Keywords: fatigue design, shaft stress analysis, shaft failure analysis. ASME code, DE-Goodman code.

1. Introduction

Shafts are critical components in the construction of machines, particularly rotating machines. They generally transmit power or rotary motion to other parts [1]. In most cases, they are circular and do not have uniform diameters [2-3].

Shafts support different power elements. Therefore, they are subjected to stresses and strains according to their assigned role. They operate under fluctuating loads or combined torsional and bending loads. This type of loading leads to fatigue failure, one of the most common causes of failure [4-5]. Under applied loads, failures generally occur in stress concentration zones such as keyways, shoulders, etc. [6].

Failure analysis is a process of gathering and analyzing data to determine the cause of a malfunction and prevent any changes in the size or shape of a structure, machine, or component, with the associated economic and safety benefits [7], which make them incapable of satisfactorily fulfilling their intended function [8]. To prevent fatigue failure of shafts, manufacturers require a better understanding of mechanical design [9-10], stress concentration factors [11], and crack propagation mechanisms [12].

Determining the proper shaft diameter is crucial in both the design and checking phases, as it is needed to withstand various stresses. The ultimate goal is to select the reason behind a failure, often tied to the malfunction of the related mechanical system.

Consequently, numerous researchers have studied fatigue in rotating shafts [13-17]. Extensive work has been conducted to elucidate the nature of shaft fatigue failures using analytical, semi-empirical, and experimental methods [18-19].

For instance, Bonnet, [20] studied the failure mechanism of a motor shaft. In this work, the authors concluded that, in the majority of cases, the primary failure mechanism of a drive shaft is fatigue when the

load to which it is subjected is axial, torsional, bending, or (in a more realistic hypothesis) a combination of loads [21].

Childs, [22], studied two dimensioning methods: ASME and DIN 743. Unlike the ASME approach, the DIN 743 procedure does not precisely compute the minimum possible shaft diameter. DIN 743 is based on the determination of the safety factor. The two approaches yield considerable differences, resulting in

significantly different safety factors. Indeed, ASME offers safety factors ranging from 1.25 to 4.0, while DIN 743 provides only a minimum safety factor of 1.2.

Da Fonte *et al.* [23] studied the effect of constant torsion on fatigue crack growth in 7075-T6 aluminum alloy shafts subjected to rotary bending. They used fracture mechanics to examine the results using stress intensity factors developed for shaft bending and torsion. They demonstrated that fatigue crack growth would be detected under constant torsion.

Our study examines the factors contributing to the fatigue of the head shaft of a bucket elevator at the "Hdjar Soud" cement plant in Skikda, Algeria. The elevator is designed to transport cement vertically over a height of several meters. The X408 shaft studied here is a rotating element with a solid circular cross-section. It transmits power and angular motion from an electric motor and reducer to the cement bucket wheel.

Following a failure during the shafts service life, we conducted a thorough visual examination of the fracture surface, which revealed that it failed due to fatigue. Subsequently, we drove further research to analyze the various modes of failure that the shaft could have experienced to identify the causes.

The work described here is based on verifying the dimensions of the drive shaft, from which we calculated the bending and torsional moments to deduce the shaft diameter by two methods:

The first is based on ASME (American Society of Mechanical Engineers) criteria. The latter is simple and helpful in design for rapid assessment of shaft diameter [24-25]. The second is based on the DE-Goodman criterion, which considers mean and alternate stress values. Various methods can be employed based on either strength or deformation criteria or the shaft's critical rotation speed.

2. Methodology

Fatigue failure can occur due to a defect introduced during manufacturing or degradation of the shaft during service. In this study, we present the findings of a failure analysis of a bucket elevator drive shaft that failed before reaching its expected service life limit.

2.1. System description

2.1.1. The bucket elevator

The bucket elevator is commonly used in the cement industry (Fig.1 it is designed to convey cement continuously and vertically from a height of around $30\ m$ at a conveying rate of up to $500\ T/H$ for storage in silos. In this system, cement is loaded through a hopper at the base. The hopper continuously feeds the cement into buckets evenly spaced on a chain. The chain is attached to a sprocket wheel connected to the drive shaft we are studying. The buckets are designed to pick up the cement as they move along the chain.

2.1.2. The elevator drive shaft

The failed shaft under investigation was the head or drive shaft of the elevator (coded X408 at the factory), an essential part of the elevator. It rotates at a low, almost constant speed of about $40\ m/mn$ and is supported by bearings. It transmits rotary motion, torque, and power from an electric motor 1 ($Pm = 110\ KW\ ,\ Nm = 1485\ rpm$), motion is transmitted through hydraulic coupling 2 to the reducer 3 and finally to the double chain wheel four via coupling 4 (Fig.1)

Since it is known that most shaft failures are caused by fatigue, it is recommended that at the design stage, shafts are correctly dimensioned to avoid fatigue failures during the period of use foreseen by the industry. It must be engineered to withstand static and cyclic loads to ensure optimal shaft functionality over its service life. The cyclic load, borne by the shaft, induces bending and generates stresses within the shaft that may result in fatigue failure, even if the stress amplitude falls below the material's yield strength. The following image (Fig.2) depicts the 3D shape of the shaft.

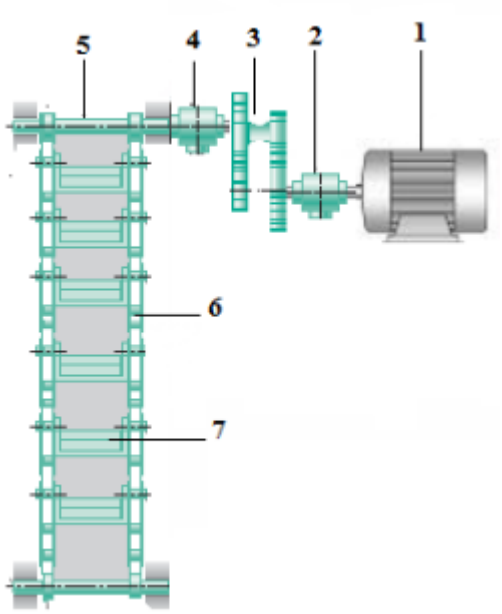


Fig.1. Diagram illustrating the shaft's location in the elevator's upper part: 1 – electric motor, 2+4 – coupling, 3 – reducer, 5 – drive shaft, 6 – chain, 7 – buckets.



Fig.2. 3D shaft illustration.

3. Materials and methods

3.1. Shaft material

Power transmission shafts are commonly made from low- or medium-carbon steel, which can be hot-rolled, cold-drawn, or forged. Materials such as *1040* or *1045* steel are frequently used.

Table 1. Chemical composition of AISI 1045.

C%	Si%	Mn%	P%	S%
0.42 – 0.48	*0.15 – 0.35*	*0.60 – 0.90*	*0.03*	*0.035*

Table 2. Mechanical properties of AISI 1045 [26].

Poisson ratio	**Yield strength** $[MPa]$	**Fracture strength** $[MPa]$	**Elastic moduls** $[GPa]$	**Density** $\left[kg/m^3\right]$
0.27 – 0.30	*343 – 490*	*569 – 686*	*190 – 210*	*7700 – 8030*

AISI 1045 steel is the material considered for the drive shaft of our elevator. It is commonly used for posts due to its high rigidity, excellent dimensional accuracy, and good strength (especially fatigue strength). Its chemical characteristics are shown in Tab.1.

The Tab.2 summarizes some of the mechanical properties of AISI 1045 steel.

3.2. Shaft force modeling

A beam with a rectilinear mean line models the drive shaft. The arrangement and nature of the elements making the pivot connection between the shaft and the frame are well-known, as are the forces applied by the various components with which it is linked. Assuming that we're dealing with a combination of bending and torsion loads and considering the shaft as a beam, as illustrated in Fig.3.

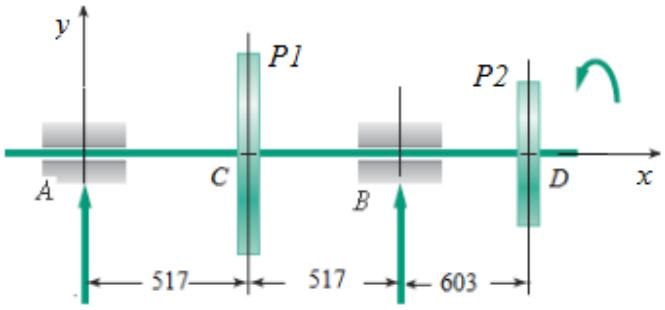


Fig.3. Scheme of the proposed shaft showing loads and nominal dimensions.

Based on the fundamental principle of statics, we calculated the head shaft's reaction forces (R) and moments (M). This shaft supports not only its weight, which is $2100\,kg$, but also the total weight of the chain, the buckets, and the cement material it carries. Additionally, it bears the weight of the coupling on the right.

$$\sum F = 0, \tag{3.1}$$

$$\sum M = 0. \tag{3.2}$$

Table 3. Various loads and moments are applied to the drive shaft.

Symbol	Description	Values
RA	Reaction at bearing on side point A, $[N]$.	*53002*
RB	Reaction at bearing on other side point B, $[N]$.	*78998*
P1	Load applied to the middle of support point C, $[N]$.	*120000*
P2	Load applied to shaft end on right point D, $[N]$.	*12000*
Mf	Maximum bending moment, $[Nm]$.	*7236*
T	Maximum torque on shaft, $[Nm]$.	*21497*

Assuming that the reducer has the following characteristics:

$$N = 40\,rpm, \quad P = 90\,kW.$$

The maximum applied torque T is calculated using Eq.(3.3):

$$T = \frac{P}{\omega} = \frac{30\ P}{\pi.N}. \tag{3.3}$$

The following table summarizes the calculated values of various loads and moments applied to the shaft:

4. Results and discussion

4.1. Selection and use of failure theories

During the bucket elevator system running, the drive shaft is subjected to the torque of the motor and the bending moment of the weight of the wheel, the cement-filled buckets, and the weight of the shaft itself. These generate torsional shear and bending stresses on the shaft [27]. Therefore, the shaft has been designed to avoid fatigue failure during its intended period of use while ensuring its correct dimensioning.

There are several methods for calculating shaft diameter or verifying shaft strength. The accuracy of reliable methods may vary based on several factors. Two approaches are available. The accuracy of reliable methods may vary based on several factors. Two approaches are available:

1. ASME code approach, also known as B106.1M-1985.
2. Energy distortion theory (DE-Goodman method).

4.2. Calculating minimum diameter

4.2.1 ASME method

In practice, many shaft design cases involve a simple stress state. This state is often characterized by constant shearing and torsional stress components produced by an operating torque. Additionally, a fully reversed bending stress component is generated by continuous transverse forces on the rotating shaft (ANSI/ASME, [28]). The ASME method is simple to use. It is a convenient design tool, as it enables the diameter of shafts to be rapidly estimated using a static limitation theory based on maximum shear, as described in numerous American and English works [29-30].

For a full circular shaft section, the maximum shear stress is calculated using Mohr's circle, describing the stress and strain at different planes, and the following Eq.(4.1):

$$\frac{16}{\pi d^3}\sqrt{\left(K_B M\right)^2 + \left(K_T T\right)^2} \le \sigma_{allowable}. \tag{4.1}$$

According to the steel grade AISI 1045 (C45) [31]:

$$S_y = 375\,(N/mm^2), \tag{4.2}$$

$$S_{ut} = 660\,(N/mm^2). \tag{4.3}$$

The ASME Method defines adequate stress as the smaller of the following two values:

$$\sigma_b = 0,3S_y = 0,3 \times 375 = 112,5\left(N/mm^2\right), \tag{4.4}$$

$$\sigma_b = 0,18 \times S_{ut} = 118,8 \left(N / mm^2 \right). \tag{4.5}$$

So, we consider:

$$\sigma_b = 112,5 \left(N / mm^2 \right). \tag{4.6}$$

The allowable shear stress is calculated using the following equation:

$$\sigma_{allowable} = 0.75 \times \sigma_b = 84,375 \left(N / mm^2 \right). \tag{4.7}$$

Equation (4.1) is used to determine the solid shaft diameter, given by:

$$d = \left\{ \frac{16}{\pi.\sigma_{allowable}} \left[\left(K_B M \right)^2 + \left(K_T T \right)^2 \right]^{1/2} \right\}^{1/3}. \tag{4.8}$$

Hence, the minimum diameter of the shaft will be:

$$d = 140.97 \ mm . \tag{4.9}$$

4.2.2. DE-Goodman method

In the case of shafts, there are two main sources of stress: bending and torsion. Pressures due to axial loads are frequently present but generally negligible. Assuming only bending and torsion, let M_a and M_m represent alternating and midrange bending moments, and T_a and T_m represent alternating and midrange torques.

Often, for a stable, rotating shaft (i.e., rotating at a constant speed with constant loads), the torque can be treated as regular (i.e., $T_a = 0$), and the moment can be considered as completely reversed due to shaft rotation $\left(M_m = 0 \right)$ [32-34].

In many design manuals for mechanical components, stress concentration factors for bearings with different fillets, grooves, and holes on shafts are explored and presented in sets of curves [35].

4.2.2.1. Failure criteria

Fatigue diagram (Fig.4) shows various failure criteria. For each failure criterion, a point on or "above" the corresponding line indicates failure. For example, a point on the Goodman line gives force S_m as the limiting value of σm corresponding to force S_a, which, combined with σ_m, is the limiting value of σ_a.

Despite the various failure relationships proposed for loadings, the modified Goodman line is one of the most widely used failure relationships [37]. The latter is given by the following formula:

$$\frac{1}{n} = \frac{\sigma'_a}{S_e} + \frac{\sigma'_m}{S_{ut}}. \tag{4.10}$$

For analysis purposes, it's reasonably straightforward to combine the different types of stress into alternating and midrange Von Mises stresses. Fluctuating stresses due to bending and torsion are given by:

$$\sigma_a = K_f \frac{32M_a}{\pi d^3}, \tag{4.11}$$

$$\sigma_m = K_f \frac{32M_m}{\pi d^3}. \tag{4.12}$$

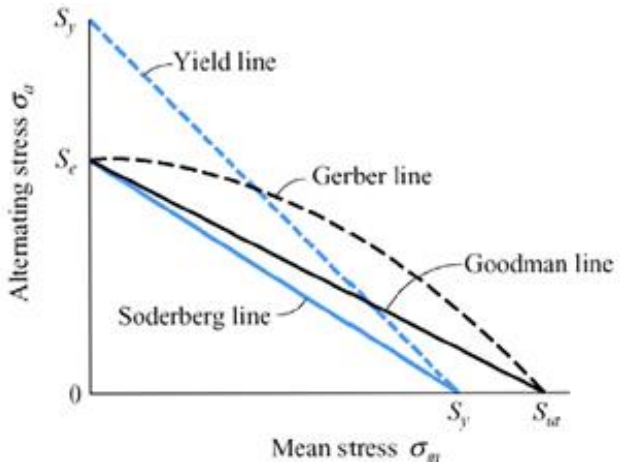


Fig.4. Fatigue diagram showing various criteria of failure [36].

According to distortion energy failure theory, the Von Mises stresses for rotating solid shafts, neglecting axial loads, can be determined by combining these stresses:

$$\sigma'_a = \left(\sigma_a^2 + 3\tau_a^2\right)^{1/2} = \left[\left(K_f \frac{32M_a}{\pi d^3}\right)^2 + 3\left(K_{fs} \frac{16T_a}{\pi d^3}\right)^2\right]^{1/2}, \tag{4.13}$$

$$\sigma'_m = \left(\sigma_m^2 + 3\tau_m^2\right)^{1/2} = \left[\left(K_f \frac{32M_m}{\pi d^3}\right)^2 + 3\left(K_{fs} \frac{16T_m}{\pi d^3}\right)^2\right]^{1/2}. \tag{4.14}$$

Moreover, substituting σ_a and σ_m from Eqs (4.11) and (4.12) leads to the following formula:

$$\frac{1}{n} = \frac{16}{\pi d^3}\left\{\frac{1}{S_e}\left[4\left(K_f M_a\right)^2 + 3\left(K_{fs} T_a\right)^2\right]^{1/2} + \frac{1}{S_{ut}}\left[4\left(K_f M_m\right)^2 + 3\left(K_{fs} T_m\right)^2\right]^{1/2}\right\}. \tag{4.15}$$

Equation (4.15) accurately estimates the diameter of a solid rotary shaft with a circular cross-section and ductile material subjected to constant torque and fully reversed bending.

The diameter (d) at the groove in the middle of the shaft was determined using the DE-Goodman criterion, as shown in Eq.(4.16), considering that the alternating torque and mean bending moment for the rotating shaft were equal to zero:

$$d = \left(\frac{16n}{\pi}\left\{\frac{2\,K_f M_a}{S_e} + \frac{\sqrt{3}K_{fs}T_m}{S_{ut}}\right\}\right)^{1/3}. \tag{4.16}$$

The stress concentration factors K_f and K_{fs} can be calculated using the following formulas:

$$K_f = 1 + q(K_t - 1) = 1 + 0,65(2,4 - 1) = 1,91, \tag{4.17}$$

$$K_{fs} = 1 + q(K_{ts} - 1) = 1 + 0,7(1,4 - 1) = 1,28. \tag{4.18}$$

These two factors depend on the geometry and loading mode. K_t and K_{ts} values are published in numerous reference works [38], and the most frequently encountered cases are illustrated in the following Tab.4.

Table 4. Values of K_t and K_{ts} factors.

	K_t	K_{ts}
$r = 0.4$	2.4	1.4
$q = 0.7$		

4.2.2.2. Determination of endurance strength

According to Marin, [39], the endurance limit *Se* for a mechanical element can be estimated by Eq.(4.19) [40]:

$$Se = C_{load}\, C_{size} C_{surf} C_{temp} C_{reliab} Se'. \tag{4.19}$$

Here, a series of modification factors are applied to the endurance limit of a test specimen for various effects such as size, load, and temperature. These factors are determined from [41].

Where:

- C_{load} – load factor,
- C_{size} – size factor,
- C_{surf} – surface factor,
- C_{temp} – temperature factor,
- C_{reliab} – reliability factor.

The approximate relationship between the endurance limit of test specimens and the ultimate tensile strength of the material (for steels only) is as follows:

$$S_{ut} = 660 < 1400MPa, \tag{4.20}$$

The endurance limit of the specimen will be:

$$S_{e'} = 0,5 \cdot S_{ut} = 0,5 \times 660 = 330N / mm^2. \tag{4.21}$$

The load coefficient is given by the equation below:

$$C_{load} = 1 \quad \text{(bending load)}. \tag{4.22}$$

The size factor can be calculated using equation (4.23) [42]:

$$C_{size} = 1,189(d)^{-0,097} = 1,189(220)^{-0,097} = 0,704\,, \tag{4.23}$$

for $8mm \le d \le 250mm$.

Thus, the area factor is calculated as follows [43]:

$$C_{surf} = B(S_{ut})^{b} = 0,426\,, \tag{4.24}$$

$$C_{temp} = 1\,, \tag{4.25}$$

for $T \le 450°C$.

$$C_{reliab} = 0,897\,. \tag{4.26}$$

The calculated correction factors are given in Tab.5.

Table 5. Calculated correction factors.

C_{load}	C_{size}	C_{surf}	C_{temp}	C_{reliab}
1	0.704	0.426	1	0.897

So: $Se = 77.88\,N/mm^2$. (4.27)

4.2.2.3. Safety factor selection

The value of a safety factor is generally based on the experience of what has given acceptable performance in the past. The level depends on the consequences of component failure and the cost of increasing safety measures. Typical values for the resistance-based safety factor recommended by Vidosek, [44] are:

$$n = 1.5 \tag{4.28}$$

Replacing n by its value in Eq.(4.16), the shaft diameter will be:

$$d = \left(\frac{16 \times 1,5}{3,14} \left\{ \frac{2 \times 1,91 \times 27402034}{88,77} + \frac{\sqrt{3} \times 1,28 \times 21496815}{660} \right\} \right)^{1/3}. \tag{4.29}$$

Then:

$d = 212.27mm$, we take: $d = 214\ mm$.

After comparing the shaft diameters calculated by the ASME and DE-Goodman methods, it is evident that the ASME method has calculated a shaft diameter of $140\ mm$, significantly different from the manufacturer's diameter. However, the computed value still falls within the acceptable range. This difference is because the manufacturer's calculation does not consider all the factors that can impact the applied stresses, whereas the ASME method accounts for more precise factors.

Nevertheless, calculation using the DE-Goodman method yielded $214\ mm$, and we note that the shaft diameter calculated by this method is very close to that of the manufacturer $(220\ mm)$, which means that the shaft can support the applied load and torque, which is appropriate for the design of the elevator.

5. Conclusion

Within this study, we present two distinct methodologies, namely ASME and DE-Goodman, designed to accurately size an elevator's drive shaft. Thus, the main objectives were as follows:

- Determine whether the shaft failure is a result of substandard design.
- Verify the steel grade resistance.
- Find the leading cause of failure.
- Avoid the same failure in the future.
- Identify the type of failure.
- Improve component quality.

It was concluded that the shaft studied had failed by fatigue, that premature failure had occurred due to a high-stress concentration in its middle at the impeller keyway, and that the load applied by the impeller and the weight of the shaft were significant.

The results showed that the diameter calculated by the DE-Goodman method $(d = 214\ mm)$ is more accurate than that obtained by the ASME method $(d = 140\ mm)$. Therefore, this method can be used as the most appropriate approach for verification purposes.

After conducting the necessary calculations, we determined that the shaft is safe and economically feasible, with an appropriate diameter for manufacturing purposes. This observation suggests that an AISI 1045 material can handle loads and stresses up to the ultimate yield strength of $375\ MPa$.

Based on our analysis, the root cause of the failure was cement blockage at the loading level of the buckets.

Acknowledgements

I would like to express my sincere thanks to the mechanical engineers at GICA for their availability, their support and for all the information, they made available to us during the period in which this work was carried out.

Nomenclature

C – Carbon
d – shaft diameter
KB – bending load coefficient
K_f, K_{fs} – the fatigue stress concentration factors for bending and torsion, respectively
K_T – torsional load coefficient
M – bending moment
M_m, M_a – the midrange and alternating bending moments
Mn – Manganes
N – rotational speed
n – factor of safety
P – Phosphorus
P – permissible power
S – Sulfur
Se – endurance limit
$Sé$ – endurance limit of test specimen
Si – Silicon

S_{ut} – ultimate tensile strength
Sy – yield strength
T – torque or torque moment
T_m, T_a – the midrange and alternating torques
σ_a – amplitude component
σ'_a, σ'_m – the Von Mises stresses
σ_m – midrange component
ω – angular rotation

References

[1] Raut S.P. and Raut L.P. (2014): *A review of various techniques used for shaft failure analysis*.– International Journal of Engineering Research and General Science, vol.2, No.2, pp.159-171.

[2] Engel B. and Al-Maeeni S.S.H. (2018): *Finite element analysis and experimental determination of a shaft deflection under three-point loading*.– Vibroengineering PROCEDIA, vol.19, No.11, pp.199-204, https://doi.org/10.21595/vp.2018.20065.

[3] Norton R.L. (2006): *Machine Design: An Integrated Approach*.– Pearson Prentice Hall, 2nd ed., Upper Saddle River, NJ, USA.

[4] Domazet Ž., Lukša F. and Bugarin M. (2014): *Failure of two overhead crane shafts*.– Engineering Failure Analysis, vol.44, pp.125-135, https://doi.org/10.1016/j.engfailanal.2014.05.001.

[5] Göksenli A. and Eryürek I.B. (2009): *Failure analysis of an elevator drive shaft*.– Engineering Failure Analysis, vol.16, No.4, pp.1011-1019, https://doi.org/10.1016/j.engfailanal.2008.05.014.

[6] Zappalorto M., Berto F. and Lazzarin P. (2011): *Practical expressions for the notch stress concentration factors of round bars under torsion*.– International Journal of Fatigue, vol.33, No.3, pp.382-395, https://doi.org/10.1016/j.ijfatigue.2010.09.016.

[7] Becker W.T. and Shipley R.J. (2002): *ASM Handbook: Failure Analysis and Prevention*.– ASM International, vol.11, Materials Park, Ohio, USA, https://doi.org/10.31399/asm.hb.v11.9781627081801.

[8] Collins J.A. (1993): *Failure of Materials in Mechanical Design: Analysis, Prediction, Prevention*.– John Wiley & Sons, 2nd ed., New York, USA.

[9] Hamrock B.J., Schmid S.R. and Jacobson B.O. (2005): *Fundamentals of Machine Elements*.– McGraw-Hill, 2nd ed., New York, USA.

[10] Darlington J.F. and Booker J.D. (2006): *Development of a design technique for the identification of fatigue initiating features*.– Engineering Failure Analysis, vol.13, No.7, pp.1134-1152, https://doi.org/10.1016/j.engfailanal.2005.07.006.

[11] Noda N.A., Takase Y. and Monda K. (1997): *Stress concentration factors for shoulder fillets in round and flat bars under various loads*.– International Journal of Fatigue, vol.19, No.1, pp.75-84, https://doi.org/10.1016/S0142-1123(97)82050-6.

[12] de Freitas M., Reis L. and Li B. (2011): *Effect of steady torsion on fatigue crack initiation and propagation under rotating bending: multiaxial fatigue and mixed-mode cracking*.– Engineering Fracture Mechanics, vol.78, No.5, pp.826-835, https://doi.org/10.1016/j.engfracmech.2009.12.012.

[13] Shih Y.S. and Chen J.J. (1997): *Analysis of fatigue crack growth on a cracked shaft*.– International Journal of Fatigue, vol.19, No.6, pp.477-485, https://doi.org/10.1016/S0142-1123(97)00062-8.

[14] Lin X.B. and Smith R.A. (1998): *Fatigue growth simulation for cracks in notched and unnotched round bars*.– International Journal of Mechanical Sciences, vol.40, No.5, pp.405-419, https://doi.org/10.1016/S0020-7403(97)00039-8.

[15] Suga K., Kikuchi M., Wada Y. and Kawai H. (2017): *Study on fatigue growth of multi-surface flaws in shaft under rotary bending by S-FEM*.– Engineering Fracture Mechanics, vol.174, pp.207-214, https://doi.org/10.1016/j.engfracmech.2016.11.001.

[16] Daemi N. and Majzoobi G.H. (2011): *Experimental and theoretical investigation on notched specimens life under bending loading*.– International Journal of Mechanical and Mechatronics Engineering, vol.5, No.8, pp.1639-1643.

[17] Prasad S.R. and Sekhar A.S. (2018): *Life estimation of shafts using vibration based fatigue analysis*.– Journal of Mechanical Science and Technology, vol.32, No.9, pp.4071-4078, https://doi.org/10.1007/s12206-018-0806-4.

[18] Rice R.C., Leis B.N. and Nelson D.V. (1988): *Fatigue Design Handbook*.– Society of Automotive Engineers (SAE International), 3rd ed., Warrendale, PA, USA.

[19] Osgood C.C. (1982): *Fatigue Design*.– Pergamon Press, 2nd ed., Oxford, UK.

[20] Bonnet A.H. (1998): *Cause, analysis and prevention of motor shaft failures*.– IEEE Industrial and Commercial Power Systems Technical Conference, pp.166-180, https://doi.org/10.1109/PAPCON.1998.685518.

[21] Xu X., Yu Z. and Ding H. (2006): *Failure analysis of diesel engine gear shaft*.– Engineering Failure Analysis, vol.13, No.8, pp.1351-1357, https://doi.org/10.1016/j.engfailanal.2005.10.003.

[22] Childs P.R.N. (2004): *Mechanical Design*.– Elsevier Butterworth-Heinemann, 2nd ed., Oxford, UK.

[23] Fonte M., Reis L. and de Freitas M. (2014): *The effect of steady torsion on fatigue crack growth under rotating bending loading on aluminium alloy 7075-T6*.– Frattura ed Integrità Strutturale, vol.8, No.30, pp.360-368, https://doi.org/10.3221/IGF-ESIS.30.43.

[24] Shigley J.E., Mischke C.R. and Budynas R.G. (2004): *Mechanical Engineering Design*.– McGraw-Hill, 7th ed., New York, USA.

[25] Hamrock B.J., Jacobson B.O. and Schmid S.R. (1999): *Fundamentals of Machine Elements*.– McGraw-Hill, 1st ed., Boston, USA.

[26] Davis J.R. (1998): *Metals Handbook Desk Edition*.– ASM International, 2nd ed., Materials Park, Ohio, USA.

[27] Xu X. and Yu Z. (2009): *Failure analysis of a locomotive turbo-charger main shaft*.– Engineering Failure Analysis, vol.16, No.1, pp.495-502, https://doi.org/10.1016/j.engfailanal.2008.06.007.

[28] ANSI/ASME (1985): *Design of Transmission Shafting*.– American National Standards Institute / ASME, Standard B106.1M, New York, USA.

[29] Childs P.R.N. (1998): *Mechanical Design*.– Arnold, London, UK.

[30] Grounds J.D. (1976): *An Empirical Design Procedure for Shafts with Fatigue Loadings*.– Report DARCOM-ITC-02-08-76-017, Darcom Intern Training Center, Texarkana, TX, USA.

[31] Chevalier A. (2004): *Guide du Dessinateur Industriel*.– Hachette Technique, Paris, France.

[32] Marudachalam M.G., Kanthavel K. and Krishnaraj R. (2011): *Optimization of shaft design under fatigue loading using Goodman method*.– International Journal of Scientific & Engineering Research, vol.2, No.8, pp.1-5.

[33] Spotts M.F. (1985): *Design of Machine Elements*.– Prentice-Hall, 6th ed., Englewood Cliffs, NJ, USA.

[34] Shigley J.E. and Mischke C.R. (1989): *Mechanical Engineering Design*.– McGraw-Hill, 5th ed., New York, USA.

[35] Mott R.L. (2004): *Machine Elements in Mechanical Design*.– Pearson Prentice Hall, 4th ed., Upper Saddle River, NJ, USA.

[36] Hamrock B.J., Schmid S.R. and Jacobson B.O. (2005): *Fundamentals of Machine Elements*.– McGraw-Hill, 2nd ed., New York, USA.

[37] Budynas R.G. and Nisbett J.K. (2010): *Shigley's Mechanical Engineering Design*.– McGraw-Hill, 9th ed., New York, USA.

[38] Peterson R.E. (1951): *Design factors for stress concentration*.– Machine Design, vol.23, No.5, pp.159-161.

[39] Marin J. (1962): *Mechanical Behavior of Engineering Materials*.– Prentice-Hall, Englewood Cliffs, NJ, USA.

[40] Shigley J.E. (1986): *Mechanical Engineering Design*.– McGraw-Hill, Metric ed., New York, USA, pp.242-256.

[41] Mischke C.R. (1987): *Prediction of stochastic endurance strength*.– Journal of Vibration, Acoustics, Stress, and Reliability in Design, vol.109, No.1, pp.113-122, https://doi.org/10.1115/1.3269395.

[42] Mischke C.R. (1987): *Prediction of stochastic endurance strength*.– Journal of Vibration, Acoustics, Stress, and Reliability in Design, vol.109, No.1, pp.113-122, https://doi.org/10.1115/1.3269395.

[43] Kuguel R. (1961): *A relation between theoretical stress concentration factor and fatigue notch factor deduced from the concept of highly stressed volume*.– Proceedings of the ASTM, vol.61, pp.732-748.

[44] Vidosek J.P. (1957): *Machine Design Projects*.– Ronald Press Company, New York, USA.

Received: August 19, 2025
Revised: June12, 2026